

## -Supplementary Information-

### A new thin layer cell for battery related DEMS-experiments:

#### The activity of redox mediators in the Li-O<sub>2</sub> cell

P. P. Bawol<sup>a</sup>, P. Reinsberg<sup>a</sup>, C. J. Bondue<sup>a</sup>, A. A. Abd-El-Latif<sup>a,b</sup>, P. Königshoven<sup>a</sup> and H. Baltruschat<sup>a\*</sup>

<sup>a</sup> Institut für Physikalische und Theoretische Chemie, Universität Bonn, Römerstraße 164, D-53117 Bonn, Germany

<sup>b</sup> National Research Centre, Physical Chemistry Dept., El-Bohouth St., Dokki, 12311 Cairo, Egypt

\*Corresponding author: [baltruschat@uni-bonn.de](mailto:baltruschat@uni-bonn.de)

#### 1.1. Relation between oxygen partial pressure and ionic current of mass 32

In the presented thin layer cell the saturation of oxygen within the electrolyte is determined through the applied partial pressure of oxygen. According to *Hernry`s Law* the equilibrium concentration of dissolved oxygen within the chosen electrolyte in the thin layer cell is proportional to the pressure. Therefore, the flux of oxygen into the mass spectrometer also has to be proportional to the oxygen pressure. To give a more detailed illustration, the concentration profile of the oxygen species within the thin layer cell is shown in Figure S 1.

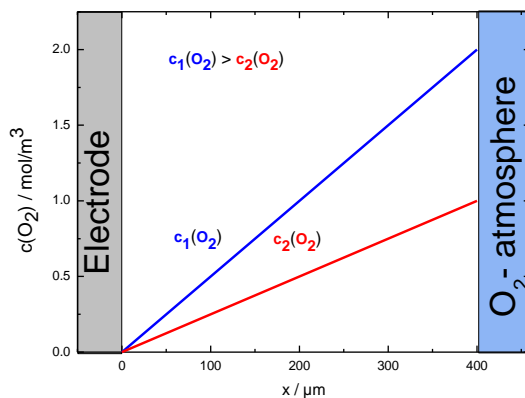


Figure S 1: Schematic representation of the oxygen concentration profile along the thickness of the working electrode compartment.

23 After an equilibrium phase, the concentration profile show a linear trend. At the boundary to  
24 the oxygen atmosphere the concentration of oxygen within the electrolyte is given by *Hernry`s*  
25 Law (we assume that there is an equilibrium at the gas/electrolyte interface).

$$c_{O_2} = k_H \cdot p_{O_2} \quad (1)$$

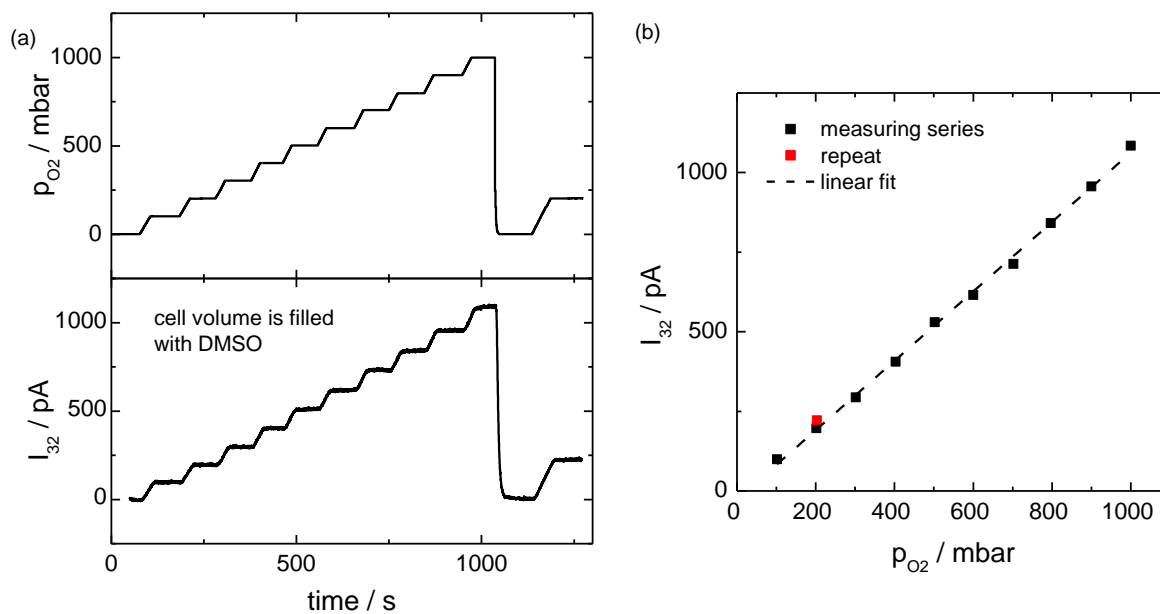
26 Because we are using a gold sputtered porous PTFE membrane as working electrode in all  
27 experiments, the dissolved oxygen is evaporating into the vacuum of the mass spectrometer.  
28 Therefore, the concentration of oxygen at the electrode-vacuum boundary is zero. The flux of  
29 oxygen into the mass spectrometer can be simply calculated by *Fick's first law*.

$$J_{O_2} = -D_{O_2} \cdot \frac{\partial c_{O_2}}{\partial x} \quad (2)$$

30 For a linear concentration profile, the term  $\frac{\partial c}{\partial x}$  simplifies to  $\frac{\Delta c}{\Delta x}$ . Taking into account that  $\Delta x$  is the  
31 thickness of the working electrode compartment as shown in Figure S 1 the term ,  $\frac{\Delta c}{\Delta x}$  can be  
32 further simplified to  $\frac{c_{O_2}}{\Delta x}$ . Combining all these simplifications into eq. (1) and eq. (2) will finally  
33 lead to eq. (3).

$$J_{O_2} = -D_{O_2} \cdot \frac{k_H \cdot p_{O_2}}{\Delta x} \quad (3)$$

34 Eq. (3) implies a proportionality between the flux of oxygen into the vacuum of the mass  
35 spectrometer and the applied partial pressure of oxygen to saturate the electrolyte with oxygen.  
36 To test the applicability of the above equations experimentally, we varied the partial pressure  
37 of oxygen to saturate the DMSO filled thin layer cell with oxygen. Simultaneously the ionic  
38 current of mass 32  $I_{32}$  was recorded (see Figure S 2 (a)). This ionic current is proportional to  
39 the flux of oxygen into the mass spectrometer. Indeed, we found the proportionality between  
40  $I_{32}$  ( $J_{O_2}$ ) and  $p_{O_2}$  as can be seen in Figure S 2 (b).

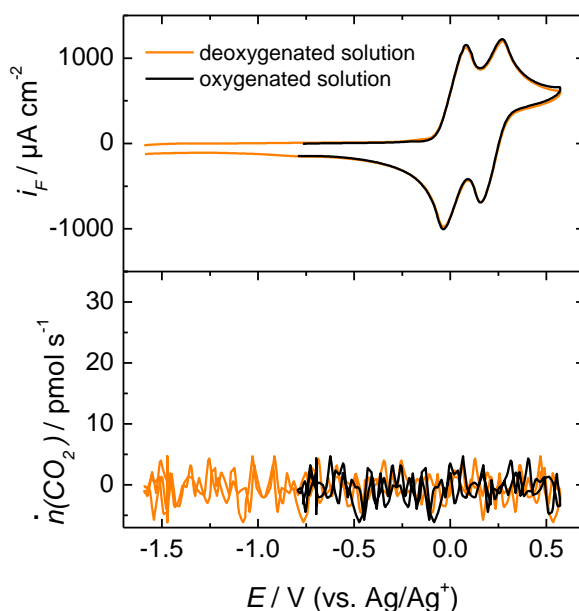


41  
 42 Figure S 2: (a): Applied oxygen partial pressure to saturate DMSO within the thin layer cell with oxygen (upper figure).  
 43 Simultaneously recorded ionic current of mass 32 (lower figure). This figure shows the time development of both  
 44 measurements. (b) Plot of the ionic current as function of the partial pressure. The plotted values were taken in the plateaus of  
 45 Figure S 2 (a). In this case the thickness of the working electrode compartment was 300  $\mu\text{m}$ .  
 46

47

## 48 1.2. Stability of TTF in deoxygenated solution

49 The measurement shown in Figure S 3 shows that there is no effect on the cyclic voltammetry  
50 response of TTF in a deoxygenated solution to an oxygenated solution. In the measurement in  
51 the deoxygenated solution, the potential window was also opened to -1.6 V vs Ag|Ag<sup>+</sup>. Even at  
52 lower electrode potentials, TTF is not undergoing any redox processes. In addition, the absence  
53 of a CO<sub>2</sub> flux indicates that TTF is not undergoing a decomposition reaction, which is releasing  
54 CO<sub>2</sub>.



55  
56 Figure S 3 CV of 10 mM TTF in a 0.5 M LiClO<sub>4</sub> in DMSO in a deoxygenated solution (orange traced) and an oxygenated  
57 solution (black traced). The lower graph shows the simultaneously recorded CO<sub>2</sub> flux. The measurements were performed  
58 with a sweep rate of 50 mV/s.

## 59 1.3. Determination of the number of electrons during the OER for RM containing 60 electrolytes

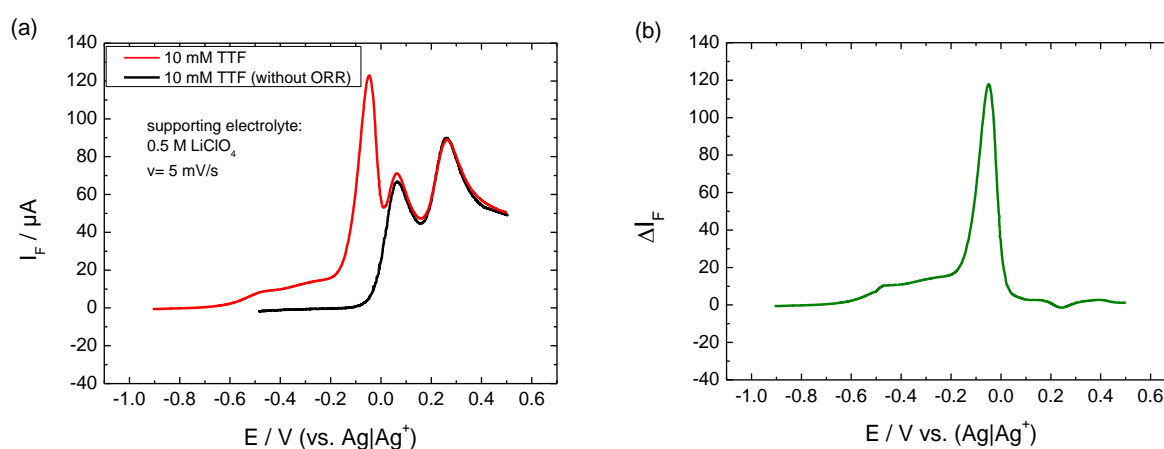
62 During the OER, the measured faradaic current consists of three different processes:

- 63 1. Direct oxidation of Li<sub>2</sub>O<sub>2</sub> on the electrocatalyst surface.
- 64 2. Oxidation of Li<sub>2</sub>O<sub>2</sub> through RM<sup>+</sup> followed by an oxidation of RM to RM<sup>+</sup> on the  
65 electrocatalyst surface.

66 3. Oxidation of  $RM$  to  $RM^+$  on the electrocatalyst surface, followed by a diffusion process  
67 of  $RM^+$  into the electrolyte without oxidizing any  $Li_2O_2$ .

68 To determine the numbers of transferred electrons per oxygen molecule for the OER processes  
69 (first and second process), the overall faradaic current has to be corrected for the contribution  
70 of the third process. Here we will briefly describe the correction procedure choosing the TTF  
71 containing experiments shown in Figure 3 (a) of our publication as an example.

72 First of all, a part of the anodic sweep in the TTF containing supporting electrolytes is taken for  
73 the analysis. The measurements shown in Figure S 4 (a) differ in their lower potential limit,  
74 which was chosen in the experiment. In the black traced measurement, the lower limit was set  
75 at  $-0.5$  V. Therefore, no ORR takes place. In the red traced measurement, the lower limit was -  
76  $1.6$  V. Since in the red traced measurement the potential was low enough to perform the ORR,  
77 one is able to observe all three processes, which were mentioned above, during the anodic  
78 sweep. On the other hand, the black traced measurement only contains the third process, as  
79 mentioned above. To isolate the OER processes, one can subtract the black traced measurement  
80 from the red traced measurement. The resulting current  $\Delta I_F$  is shown in Figure S 4 (b).  $\Delta I_F$  is  
81 further correlated with the ionic current of mass 32 to get the number of transferred electrons  
82 per oxygen molecule.

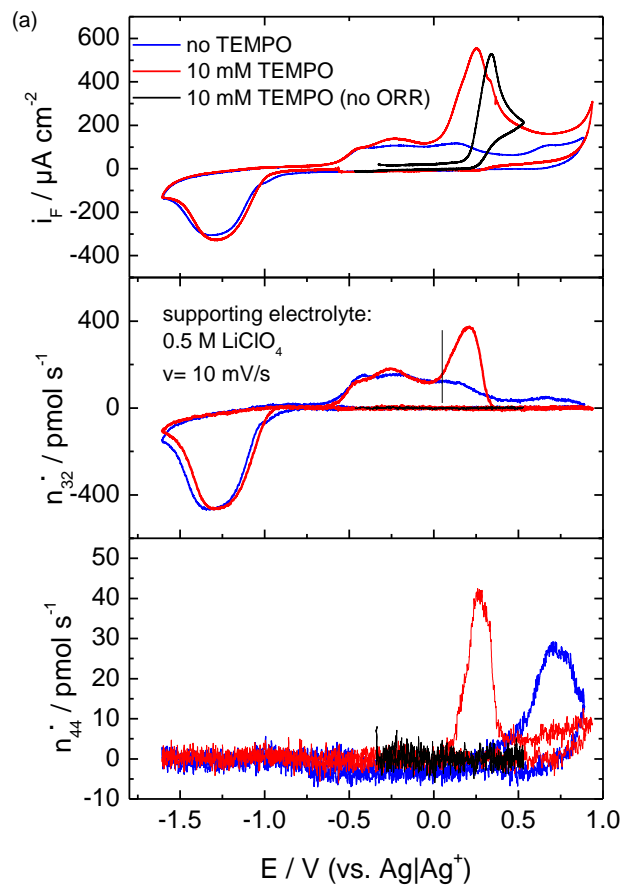


83 Figure S 4 (a): Extract of the anodic sweep for the TTF containing 0.5 M LiClO<sub>4</sub> in DMSO. For the red curve the potential was  
84 previously cycled into the ORR-region. In the black traced measurement the ORR potential region was avoided. (b): Current  
85 profile obtained out of the difference of the currents shown in (a).

86

87 **1.4. Using TEMPO as redox mediator**

88 2,2,6,6-Tetramethylpiperidinyloxy (TEMPO) was used as a redox mediator. The cyclic voltammetry  
89 and the MSCVs of mass 32 and 44 are shown in Figure S 5. It is remarkable that for the DMSO based  
90 electrolyte, we observe an irreversible TEMPO-redox system. The previous article including TEMPO  
91 as redox mediator in Li-O<sub>2</sub> cells were performed in Tetraglyme based electrolytes[1, 2]. Nevertheless,  
92 this experiment was used to determine the potential at which the activity of the redox mediator starts as  
93 well as the half wave potential of the TEMPO oxidation peak.

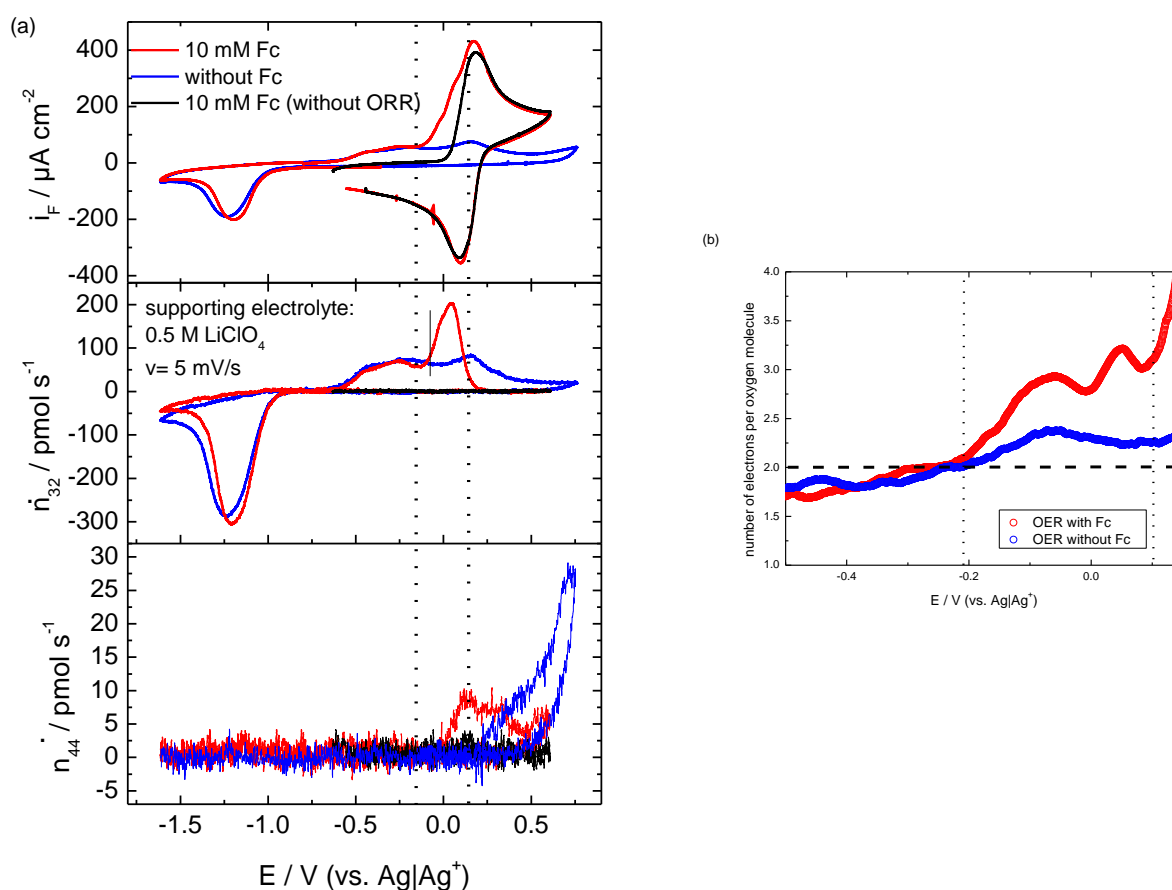


94  
95 Figure S 5 (a): CVs and MSCVs on mass 32 and 44 with a sweep rate of 5 mV/s in 0.5 M LiClO<sub>4</sub> solution in DMSO with  
96 10 mM TEMPO (black and red trace) and without TEMPO (blue trace).

97

## 98 1.5. Using Fc as a redox mediator

99 Ferrocenium (Fc) was also used as a redox mediator. The cyclic voltammetry and the MSCVs of mass  
100 32 and 44 are shown in Figure S 5 (a). It is well known, that the  $\text{Fc}^+$  is very sensitive to small amounts  
101 of oxygen [3]. Therefore, the black traced measurement was performed without oxygen (system to  
102 saturate the electrolyte with gas was evacuated). For the red traced measurement, the ORR was  
103 performed under an oxygen partial pressure of 900 mbar. During the anodic sweep, at a potential of -  
104 0.5 V, the potential was kept. The tubes with the oxygen atmosphere were evacuated under potential  
105 control. Afterwards, the anodic sweep was continued. The calculated number of transferred electrons  
106 per oxygen molecule are shown in Figure S 6 (b).



107  
108 Figure S 6 (a): CVs and MSCVs on mass 32 and 44 with a sweep rate of 5 mV/s in 0.5 M  $\text{LiClO}_4$  solution in DMSO with  
109 10 mM Fc (black and red trace) and without Fc (blue trace). (b) Calculated number of transferred electrons per oxygen molecule  
110 z.

111

112

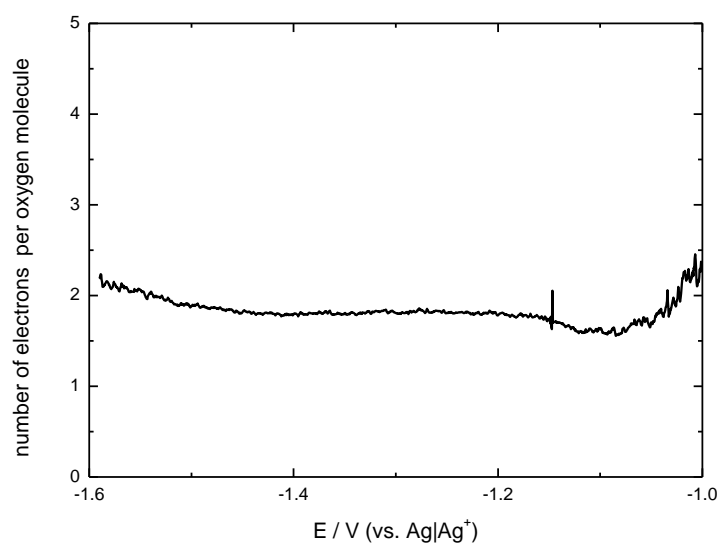


113

## 114 1.6. Number of transferred electrons during the ORR

115 The typical number of electrons, which we observe during the ORR in DMSO based  
116 electrolytes is shown in Figure S 7. Our work group previously reported about this observation  
117 [4].

118



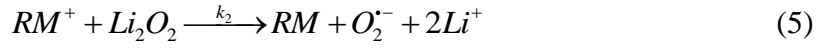
119

120 Figure S 7: Number of electrons transferred per oxygen molecule during the ORR for a 0.5 M LiClO<sub>4</sub> in DMSO.

121

122 **1.7. A thermodynamic and kinetic analysis of the Li<sub>2</sub>O<sub>2</sub> oxidation through a redox**  
 123 **mediator**

124 In our analysis, the following chemical and electrochemical reactions were considered:



125 In this reaction scheme it is reasonable to assume that the reaction (5) is the rate determining  
 126 step. According to reaction (5), the  $O_2^{\bullet -}$  production rate can be formulated as followed:

$$\frac{d[O_2^{\bullet -}]}{dt} = k_2 [Li_2O_2] [RM^+] \quad (8)$$

127 Expressing the concentration of  $RM^+$  through Nernst law leads to:

$$\frac{d[O_2^{\bullet -}]}{dt} = k_2 [Li_2O_2] [RM] \cdot e^{-(E - E_{RM/RM^+}^0)F/RT} \quad (9)$$

128 In equation (9)  $E$  stands for the electrode potential and  $E_{RM/RM^+}^0$  for the standard potential of

129 RM. Including the initial concentration of RM,  $[RM_0]$ :

$$[RM_0] = [RM] + [RM^+] \quad (10)$$

130 This leads to the following expression:

$$\frac{d[O_2^{\bullet -}]}{dt} = k_2 [Li_2O_2] [RM_0] / (1 + e^{-(E - E_{RM/RM^+}^0)F/RT}) \quad (11)$$

131 In the next step we assumed that the rate constant  $k_2$  is given by Marcus' expression:

$$k_2 = k_{2,0} \exp\left(-\frac{(\lambda + \Delta G_0)^2}{4\lambda RT}\right) \quad (12)$$

132 Where  $\lambda$  is the reorganization energy and  $\Delta G_0$  the free enthalpy of the electron transfer.

133 With the help of reaction (5)  $\Delta G_0$  can be expressed as follows:

$$\Delta G_0 = -F \left( E_{RM^+/RM}^0 - E_{Li_2O_2/O_2^-}^0 \right) = -FE_R \quad (13)$$

134 Combing equation (12) and (14) results in:

$$k_2 = k_{2,0} \exp \left( -\frac{\lambda}{4RT} + FE_R \left( \frac{1}{2RT} - \frac{FE_R}{4\lambda RT} \right) \right) \quad (14)$$

135 For DMSO one can assume a reorganization energy of 80 kcal/mol [5].  $E_R$  is for the  
136 investigated redox mediators between 0.7 V and 1.1 V. Taking these numbers into account, one

137 can neglect  $\frac{FE_R}{4\lambda RT}$  over  $\frac{1}{2RT}$ . Overall expression (14) simplifies to the following expression:

$$k_2 \approx k_{2,0} \exp \left( -\frac{\lambda}{4RT} + \frac{FE_R}{2RT} \right) \quad (15)$$

138 If the reaction should be an inner sphere reaction, the factor  $\frac{1}{2}$  in the second term of the

139 exponent would have to be replaced by a factor  $\alpha$  similar to that in the Butler Volmer  
140 equation.

141 Combing equation (11) and (15) leads to:

$$\frac{d[O_2^{\cdot-}]}{dt} = k_{2,0} \exp \left( -\frac{\lambda}{4RT} + \frac{FE_R}{2RT} \right) [Li_2O_2][RM_o] \cdot \left( 1 + \exp \left( \frac{-(E - E_{RM^+/RM^+}^0)F}{RT} \right) \right)^{-1} \quad (16)$$

142 Taking the logarithm and summing up all constant values as *const* gives the following

143 expression:

$$\ln \left( \frac{d[O_2^{\cdot-}]}{dt} \right) = const. + \frac{FE_R}{2RT} - \ln \left( 1 + \exp \left( \frac{-(E - E_{RM^+/RM^+}^0)F}{RT} \right) \right) \quad (17)$$

144 Our experiments showed, that the difference  $E - E^0$  is in the range between 60 mV and

145 200 mV. Therefore, the 1 in the right hand side logarithm term of equation (17) can be

146 excluded giving the following equation:

$$\ln \left( \frac{d[O_2^{\cdot-}]}{dt} \right) = const. + \frac{FE_R}{2RT} - \frac{-(E - E_{RM^+/RM^+}^0)F}{RT} \quad (18)$$

$$\frac{RT}{F} \ln \left( \frac{d[O_2^{\cdot-}]}{dt} \right) = \text{const2.} + \frac{1}{2} E_{RM/RM^+}^0 + (E - E_{RM/RM^+}^0) \quad (19)$$

147 In equation (19) the expression for  $E_R$ , defined in equations (13) and (14), was used. The  
 148 resulting term  $-\frac{E_{Li_2O_2/O_2^{\cdot-}}^0}{2}$  was included into *const.* giving *const2.*.

149 To explain the trend shown in Figure 5, equation (19) was rearranged as followed:

$$E = \frac{1}{2} E_{RM/RM^+}^0 + \text{const2.} + \ln \left( \frac{d[O_2^{\cdot-}]}{dt} \right)_E \frac{RT}{F} \quad (20)$$

150 The term  $\ln \left( \frac{d[O_2^{\cdot-}]}{dt} \right)_E$  is constant, due to our determination of E: E is the potential at which

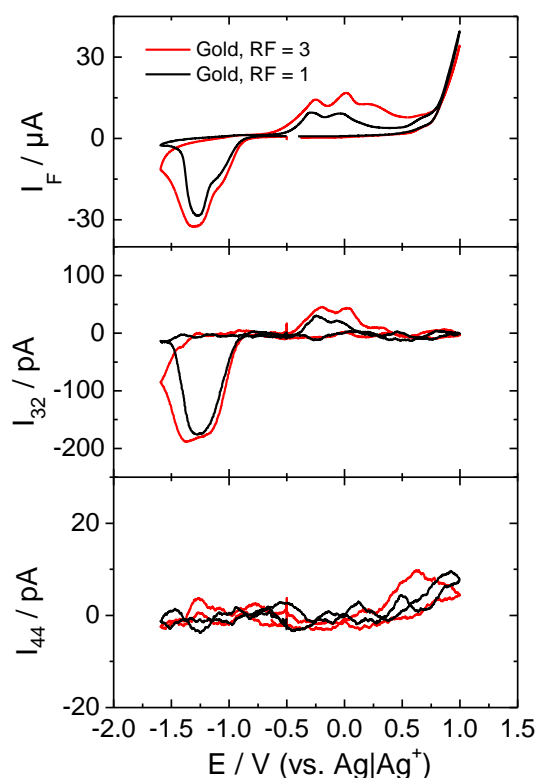
151 the oxygen flux into the mass spectrometer in the RM-containing experiment is increased over  
 152 5 pmol s<sup>-1</sup> above that observed in the measurement in the supporting electrolyte. If one assumes  
 153 that the chemical side reactions of  $O_2^{\cdot-}$  are negligible,  $O_2^{\cdot-}$  will be oxidized by a following  
 154 electrochemical reaction resulting into the oxygen flux into the mass spectrometer. Thus, E in  
 155 formula (19) is the same as the used  $E_{\text{onset}}$  within the discussion of the underlying paper of this  
 156 supporting information.

157 All in all, our combination of the Marcus' expression as well as a Nernstian behavior for the  
 158 examined oxidation of the  $Li_2O_2$  by a redox mediator shows that one would expect in a plot of  
 159  $E_{\text{onset}}$  as a function of the redox potential of the redox mediator a slope of 0.5.

160

## 161 1.8. The effect of the surface roughness on the ORR at Au-electrodes

162  
163 To examine the roughness effect of Au-surfaces on the ORR DEMS studies in a dual thin layer  
164 cell were performed (for details towards the experiment see [6]). A polycrystalline Au electrode  
165 with a roughness factor (RF) of 1 was used as a working electrode. After the measurements in  
166 a 0.5 M LiClO<sub>4</sub> O<sub>2</sub>-saturated DMSO electrolyte the surface of the electrode was roughened to  
167 a RF of 3 and the measurement in a 0.5 M LiClO<sub>4</sub> O<sub>2</sub>-saturated DMSO electrolyte was repeated.  
168 The RF values were determined by a method described by Trasatti and Petrii [7]. The  
169 experimental data is shown in Figure S 7.



170  
171 Figure S 8: DEMS study of Au-electrodes with two different roughness factors (RF). In red: RF= 3 and in blue RF=1. The  
172 figure shows the cyclic voltammetry data (top), the ionic current of mass 32 (middle) and the ionic current of mass 44  
173 (bottom).

174 The experimental data show, that the shape of the ORR is influenced by the different roughness  
175 factors. The transferred charge in the ORR is higher for the rougher surface. This is because the  
176 rougher surface is able to uptake more Li<sub>2</sub>O<sub>2</sub> before the poisoning of the electrode starts,  
177 because of its higher surface area. This result show that the slightly different shapes of the ORR

178 region within the underlying main manuscript could be explained through different roughness  
179 factors of the sputtered Au-electrodes.

- 180 [1] B. J. Bergner, A. Schürmann, K. Peppler, A. Garsuch and J. Janek, *Journal of the*  
181 *American Chemical Society*, **136**, 15054 (2014).  
182 [2] B. J. Bergner, C. Hofmann, A. Schürmann, D. Schröder, K. Peppler, P. R. Schreiner and  
183 J. Janek, *Physical Chemistry Chemical Physics*, **17**, 31769 (2015).  
184 [3] J. P. Hurvois and C. Moinet, *Journal of Organometallic Chemistry*, **690**, 1829 (2005).  
185 [4] C. J. Bondue, A. A. Abd-El-Latif, P. Hegemann and H. Baltruschat, *Journal of The*  
186 *Electrochemical Society*, **162**, A479 (2015).  
187 [5] B. Zhuang and Z.-G. Wang, *The Journal of Physical Chemistry B*, **120**, 6373 (2016).  
188 [6] H. Baltruschat, *J. Am. Soc. Mass Spectrom.*, **15**, 1693 (2004).  
189 [7] S. Trasatti and O. A. Petrii, *J. Electroanal. Chem.*, **327**, 353 (1992).

190  
191